MASTERARBEIT / MASTER'S THESIS

Titel der Masterarbeit / Title of the Master's Thesis

„A morphological description of the Cetartiodactyla Larynx using geometric morphometrics“

verfasst von / submitted by

Helena Tatjana Pichler, BSc

angestrebter akademischer Grad / in partial fulfilment of the requirements for the degree of

Master of Science (MSc)

Wien, 2022 / Vienna 2022

Studienkennzahl lt. Studienblatt / degree programme code as it appears on the student record sheet:	UA 066 878
Studienrichtung lt. Studienblatt / degree programme as it appears on the student record sheet:	Master Verhaltens-, Neuro- und Kognitionsbiologie
Betreut von / Supervisor:	Univ.-Prof. W. Tecumseh S. Fitch, PhD
Mitbetreut von / Co-Supervisor:	/

Abstract:

The wide variety of species displayed by the Cetartiodactyla taxon provides an opportunity to study how phylogenetic adaptations developed in different habitats. Including not only terrestrial orders, but also aquatic and semi-aquatic ones, artiodactyls have tapped into nearly every possible habitat, which modified their morphology distinctly. One of the most important organ systems in this process is the larynx. It's dual function of air way protection and sound production has conserved its shape over the course of evolution, while still changing enough to provide a transition to life under water in the case of the aquatic cetartiodactyls, cetaceans. With this study I provide the first shape analysis of 13 different cetartiodactylan larynges using geometric morphometrics. I therefore offer a description of the evolutionary changes semi-aquatic and aquatic cetartiodactyls underwent to adapt to the new medium they vocalize in. Further, I investigated which of these adaptations are due to phylogenetic development.

Zusammenfassung:

Die große Artenvielfalt der Cetartiodactyla, der Zweipaarhufer, bietet die ansonsten selten zu findende Möglichkeit zu untersuchen, wie sich phylogenetische Anpassungen in verschiedenen Lebensräumen entwickelt haben. Zu den Cetartiodactyla gehören nicht nur terrestrische, sondern auch aquatische und semiaquatische Arten. Somit sind nahezu alle möglichen Lebensräume erschlossen, was sich in der Morphologie deutlich widerspiegelt. Eines der wichtigsten Organsysteme in diesem Prozess ist der Kehlkopf (Larynx). Aufgrund ihrer Doppelfunktion als Schutz der Atemwege und zur Schallerzeugung hat den Larynx ihre Form im Laufe der Evolution beibehalten. Mit dem Übergang vom klassisch terrestrischen zu einem aquatischen Lebensstil, wie im Fall der Wale, wurde sie jedoch einem neuen evolutionärem Druck ausgesetzt, um ein Leben unter Wasser zu ermöglichen. Mit dieser Studie liefere ich die erste Formanalyse von 13 verschiedenen Kehlköpfen von Cetartiodactyla unter Verwendung geometrischer Morphometrie. Damit biete ich eine Beschreibung der evolutionären Veränderungen, die semiaquatische und aquatische Cetartiodactyla durchlaufen haben, um sich an das neue Medium, in dem sie vokalisieren, anzupassen. Außerdem habe ich untersucht, welche dieser Anpassungen auf eine phylogenetische Entwicklung zurückzuführen sind.

Introduction

Artiodactyls provide an interesting opportunity to study evolutionary adaptations to different environments. The taxon of cetartiodactyls contains a wide array of species inhabiting various terrestrial, semi-aquatic (e.g. hippopotamus and pygmy hippopotamus), and even aquatic ecosystems (i.e. cetaceans). This provides a unique opportunity to study evolutionary adaptations of organ systems from a comparative standpoint. One of the most important organ systems in adapting to a (semi-)aquatic environment is the larynx. The larynx is a very conserved organ that fulfils the dual functions of airway protection and acoustic signal production (Fitch, 2016; Schneider, 1964; Reidenberg, 2017; Titze 1994).

The Cetartiodactyla taxon includes an immense variety of species with most of them displaying certain laryngeal traits unique to them. Yet, this variety lies in the shape not in the overall build up and components of the larynx. The cartilages making up the cetartiodactylan larynx are the same as found in a typical mammalian body; those being the shield-like thyroid, the epiglottis, the ring-shaped cricoid connecting the larynx to the trachea, and paired arytenoids atop the cricoid. Additionally, a pair of smaller cartilages, the corniculate cartilages extend from the rostral arytenoid tips (Titze, 1994). Cranial to the larynx sits the hyoid bone, a thin U-shaped bone situated between tongue and larynx. The hyoid bone is connected to the thyroid cartilage via the thyrohyoid membrane attached to the superior edge of the thyroid (Loth et al., 2015). The vocal folds span between the attachment-point on the thyroid cartilage to the vocal processes of the arytenoids (Schneider, 1964). Both the mysticete and odontocete larynx morphology very much diverges from this typical plan (Reidenberg & Laitman, 1987; Reidenberg & Laitman, 1988; Hosokawa, 1950).

Certain unique laryngeal features shared by all cetaceans include an elongation of the arytenoid cartilages into rostral direction as well as an elongation of the arytenoids in a caudal direction (Reidenberg & Laitman, 1987; Reidenberg, 2017). In odontocetes the arytenoid cartilages are joined with the epiglottis, forming a tubular extension which tightly slots into the naso-pharyngeal cavity (Reidenberg & Laitman, 1987; Reidenberg, 2017). In mysticetes the epiglottis overlaps with the soft palate, connecting the nasal with the laryngeal passage (Reidenberg & Laitman, 2007). The existence of the corniculate and cuneiform cartilages in cetaceans has been a topic of discussion in whale morphology. Yet, while it has been quite widely accepted that the cuneiforms are absent, several authors have suggested that the corniculates make up the rostral part of the arytenoids, reaching into the nasopharyngeal cavity (Hosokawa, 1950; Schoenfuss et al., 2014). An interesting case in cetacean laryngeal morphology makes the cricoid. This cartilage is typically found in a signet ring shape, but in many baleen whales, as well as certain toothed whale species, it has been described as ventrally open and in the case of the latter even as more of a shield-like structure situated dorsally on the larynx. In the case of baleen whales this is thought to be due to the development of an air sac ventral to the larynx, which would otherwise have been constrained in its flexibility and volume was there the cricoid. On the other hand, no air sac can be found near the cricoid in toothed whales. An explanation for the cricoid not forming a ring in certain species is not yet found published (Benham, 1901; Hosokawa, 1950; Reidenberg & Laitman, 2008). Additional to these morphological changes the most striking adaptation compared to the classic Artiodactyla larynx is the change in vocal fold angle.

In odontocetes as well as mysticetes, the ligament suspected to be the vocal folds are situated parallel to the airflow rather than perpendicularly, as it is the case in most mammals and terrestrial Artiodactyla (Reidenberg & Laitman, 1988, Schneider, 1963). While in mysticetes and odontocetes they share the same orientation relative to the airflow, the underlying morphology differs. In odontocetes the dorsal attachment-points of the vocal folds are shifted downwards due to the caudal elongation of the arytenoids (Reidenberg & Laitman, 1988). This results in a 90° rotation relative to the typical mammalian position. In mysticetes, speaking of vocal folds stands as still controversial, since a homology has not been proven and only suggested. A coined term used for the potential homology currently is “U-fold”, due to its shape. There is no ligament spanning from the thyroid to the arytenoids, but instead between the caudal processes of the arytenoids a ligament enclosed in thick connective tissue spans rostrally along the arytenoids. This U-fold is situated parallel to the airflow. This results in a 90° rotation from the typical laryngeal pattern as well and interestingly, in comparison to the odontocetes it is the other way around. Therefore, vocal fold and U-fold rotation relative to the air flow has been achieved in both odontocetes and mysticetes; yet the underlying morphological adaptations differ (Hosokawa, 1950; Reidenberg & Laitman, 2007; Schoenfuss et al., 2014). While we do know about these changes, no study so far investigated evolutionary adaptions to the laryngeal cartilage morphology.

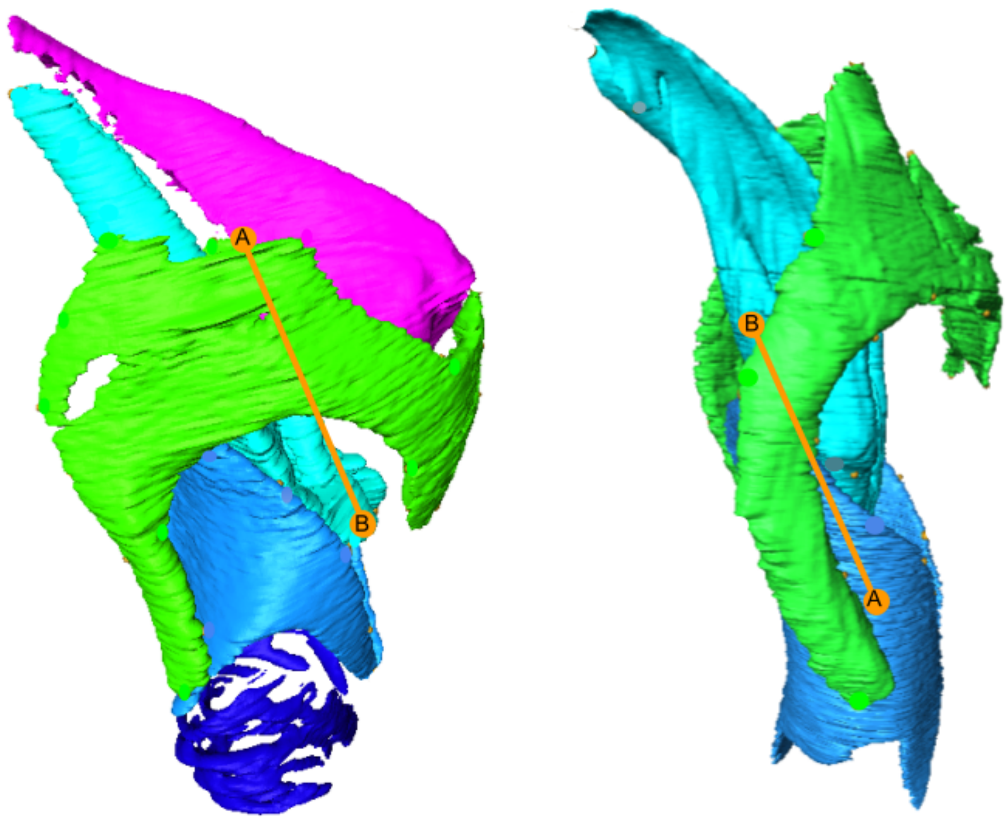

Figure 1: A schematic depiction of the position of the vocal folds of a toothed whale (*Mesoplodon bidens*) on the left, and the U-fold position in a baleen whale (*Balaenoptera borealis*) on the right. In both cases the folds are spanning from a cranial to a caudal attachment-point. They are therefore positioned parallel to the airflow. With the letter A the originally ventral attachment is indicated, with the letter B, it is the originally dorsal one. As can be seen, attachment-point A rotated in the exactly opposite direction from each specimen- in the toothed whale A developed into cranial direction, in the baleen whale towards a caudal direction.

With this study I will quantify evolutionary changes to the larynx morphology across terrestrial, semi-aquatic, and aquatic Cetartiodactyla through geometric morphometrics (GM) shape analysis. GM uses landmarks, which are morphologically relevant (structurally, developmentally or functionally) points on the organ homologous across all specimens, as a base of quantification (fixed-landmarks). The morphologically relevant surfaces, ridges and boundary curves are measured by utilizing semi-landmarks. Semi-landmarks "slide" along curves and surfaces to capture the shape between them and are therefore also called sliding landmarks. The shape analysis then is typically accomplished by the Procrustes analysis. Here the shape data of the specimens in the form of landmarks is superimposed in a common coordinate system. By then visualizing the variance of shapes between the organs, a description as well as comparison of shape changes is made possible (Richtsmeier et al., 2002; Adams & Otárola-Castillo, 2013; Gunz & Mitteroecker, 2013).

Whether these differences in shape are due to phylogenetic development inside the taxon can be measured using the indices Blomberg's K and Pagel's lambda. Both measure the phylogenetic signal, i.e. the statistical dependency of certain trait values in different species due to how they are phylogenetically related to one another. Molina-Venegas and Rodriguez (2017) have constructively criticised the use of Blomberg's K, saying it can lead to an overestimation of phylogenetic signal. Nevertheless, it is still a widely used metric and will be included in this study as well, although never without having Pagel's lambda as a possible comparison.

Methods and Materials

Specimen:

All specimens, with the exception of the sei whale and the humpback whale, here collected through the National Museums Scotland. The specimens were donated to the museum post-mortem through different European zoos and parks, as well as beach strandings (tab. 1). The larynges were excised, frozen, shipped to Vienna, and stored frozen at -20° in W. Tecumseh Fitch's lab at the University of Vienna. In the case of the minke whale and odontocetes the larynges were collected from beached cadavers through the National Museums Scotland. All specimens were post-mortem examined and no animal was killed or harmed for this study. The Sei and humpback data were provided by Coen Elemans through CT scans in the form of dicom files.

In regard to terrestrial artiodactyls I included two Camelidae (*Camelus bactrianus, Vicugnja vicugna*), two Ruminantia (*Bos taurus, Tragelaphus eurycerus*), and two Suidae (*Babyrousa babyrussa, Potamochoerus porcus*). I further included two semi-aquatic Hippopotamidae, one hippopotamus (*Hippopotamus amphibius*) and one pygmy hippopotamus (*Choeropsis liberiensis*). For aquatic artiodactyls I included two different odontocetes (*Globicephala melas, Mesoplodon bidens*) and three mysticetes (*Balaenoptera acutorostrata, Balaenoptera borealis, Megaptera novaeangliae*), leading to a total of 13 species included in this study.

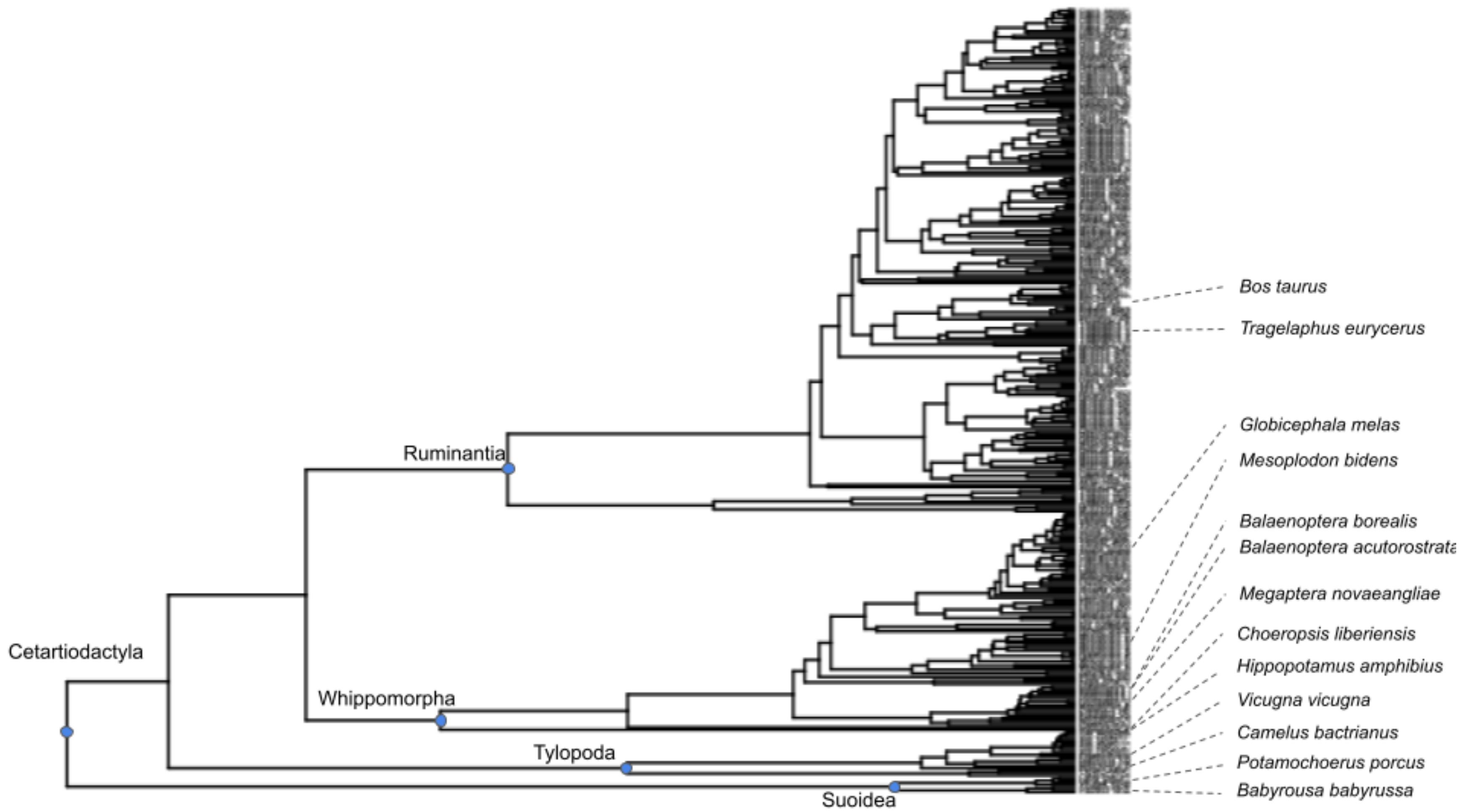

Figure 2: The Certartiodactyla Phylogeny derived from VertLife.org (Upham et al, 2019). The species included in this study are mentioned on the right. Blue dots mark the node with evolutionary splits of important monophyletic clades.

Table 1: Listed are the specimens included in this study by English and scientific name, as well as their origin.

Species name	English name	Origin	Sex
Babyrousa babyrussa	Babyrusa	Thrigby Hall Zoo	female
Balaenoptera acutorostrata	Minke whale	stranded in UK	female
Balaenoptera borealis	Sei whale	stranded in Denmark	male
Bos taurus	Cattle	National Museum Scotland Collection	female
Camelus bactrianus	Bactrian camel	National Museum Scotland Collection	female
Choeropsis liberiensis	Pygmy hippopotamus	Bristol Zoo	male
Globicephala melas	Pilot whale	stranded in UK	male
Hippopotamus amphibius	Hippopotamus	National Museum Scotland Collection	male
Megaptera novaeangliae	Humpback whale	stranded in Denmark	female
Mesoplodon bidens	Sowerby's beaked whale	stranded in UK	male
Potamochoerus porcus	Red river hog	National Museum Scotland Collection	female
Tragelaphus eurycerus	Eastern Bongo	Africa Alive Zoological Reserve	unknown
Vicugna vicugna	Vicuna	Blackpool Zoo	female

Scanning and modelling:

The frozen larynges, excluding the sei whale and the humpback whale, which were already derived as scans from the University of Southern Denmark, were scanned at the University of Veterinary Medicine in Vienna. The smaller specimens were laid out on styrofoam and covered in plastic wrap to prevent them from freezer burn until scanning. If possible, larynges were adjusted in a natural configuration pre scan. Larynges too big for any styrofoam sheet were covered in plastic wrap and scanned without any underlay. The CT scans were done with a Siemens Somatom Emotion, a 16-slice helical CT scanner, using 110-130 kV, 100-120 mAs (depending on the size of the specimen) and 0.75 mm slice thickness. The scans were reformatted in a bony and soft tissue window, with matrix size 512 x 512 and an increment of 0.6 mm, i.e. each reconstructed slice measured 512 x 512 pixels.

Larynx segmentation, 3D model reconstruction and landmark placement was performed using Amira-Avizo software (6.0 version). I segmented the thyroid, cricoid and the two arytenoids (the arytenoid-corniculate-complex in whales) but excluded the epiglottis in all specimens except the odontocetes, where the thyroid and epiglottis are partially connected. If possible, depending on the larynx and scan, one or more tracheal rings were segmented as well.

Landmarks:

All landmarks (tab. 2), fixed and sliding, were placed in Amira, using the landmarking toolkit. For the fixed landmarks I selected distinct morphological features, like maximum points of curvature (e.g. the tips of the thyroid processes). The spaces between the fixed landmarks were filled with sliding/ semi-landmarks. These were placed along the ridges and surfaces between the fixed-landmarks. Semi landmarks are not necessarily spaced evenly but are used to capture curvature between fixed landmarks. The landmark data was saved in text format for each specimen and later compiled to one complete data set, including all species.

Balaenoptera borealis (Sei whale)

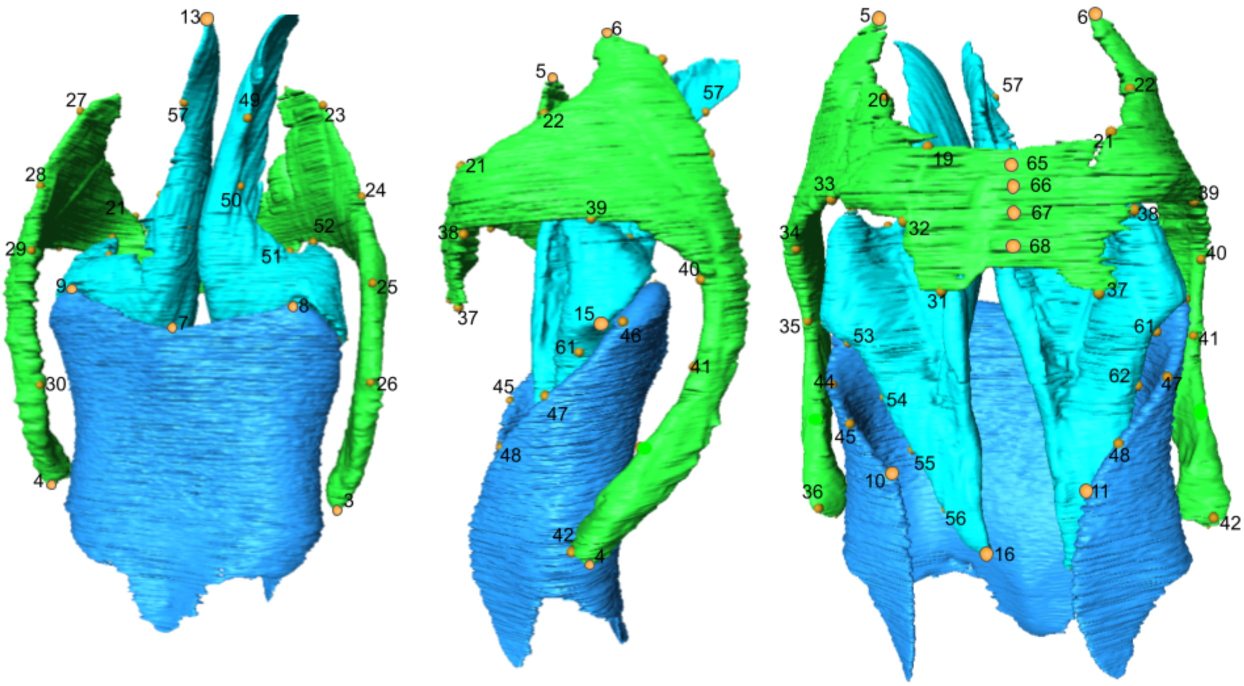

Tragelaphus eurycerus (Bongo)

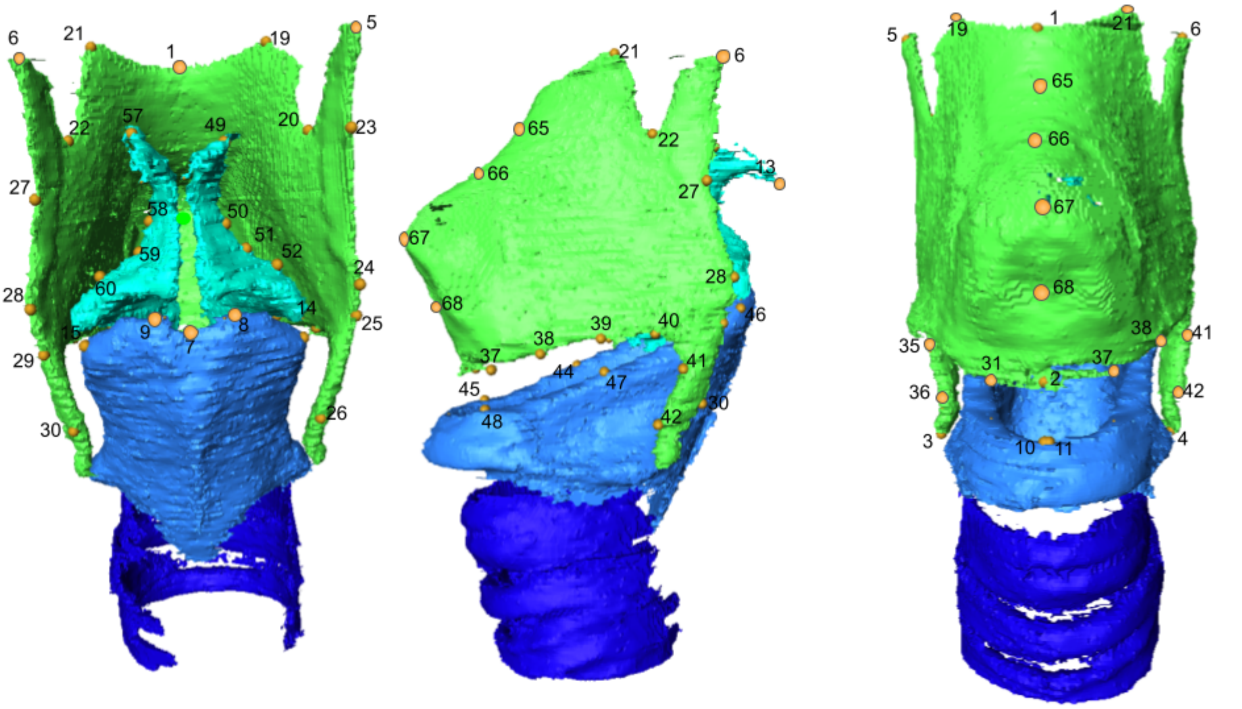

Figure 3: Depicted are three-dimensional larynx models of *Balaenoptera borealis* and *Tragelaphus eurycerus* of my data set from three perspectives. The position of the landmarks are indicated by the orange dots maked with the number of the landmark, as described in table 2.

Table 2: Listed are the 68 landmarks used in this study and their position on the larynx. In the case of the semi-/sliding landmarks it is also listed between which landmarks they slide along the model.

Landmark Nr	**cartilage**	**semi/fixed**	**Position (exact desription when seen in dorsal view with the cranial side above**	**neighboring landmark (right)**	**neighboring landmark (left)**
1	thyroid	fixed	On the ventral extend on the apical ridge placed on the midsagittal plane (thyroid)	19	21
2	thyroid	fixed	On the ventral extend on the basal ridge, also midsagitally (thyroid)	31	37
3	thyroid	fixed	On the most caudal point of the right caudal cornu (thyroid)	26	42
4	thyroid	fixed	On the most caudal point on the left caudal cornu (thyroid)	30	36
5	thyroid	fixed	On the most rostral point on the right rostral cornu (thyroid)	22	23
6	thyroid	fixed	On the most rostral point on the left rostral cornu (thyroid)	20	27
7	thyroid	fixed	On dorsal extend on apical ridge on midsagittal plane (cricoid)	8	9
8	cricoid	semi	The highest point on the dorsal apical ridge on the right (cricoid)	53	7
9	cricoid	semi	The highest point on the dorsal apical ridge on the left (cricoid)	7	46
10 (same spot as nr11 in terrestrials)	cricoid	fixed	On the ventral extend on the apical ridge on the midsagittal plane (terrestrials), in cetaceans we find the situation that the cricoid is ventrally open, therefore we chose to set the landmarks on the most apical point.	48	45
11 (same spot as nr10 in terrestrials)	cricoid	fixed	-"- in cetaceans on the left side	45	48
12	arytenoid	fixed	On the rostral processus of the right arytenoid	/	49
13	arytenoid	fixed	On the rostral processus of the left arytenoid	/	57
14	arytenoid	semi	The most lateral point of the right arytenoid	52	53
15	arytenoid	semi	The most lateral point of the left arytenoid	60	61
16	arytenoid	fixed	On the most caudal point of the vocal processus of the right arytenoid	56	/
17	arytenoid	fixed	On the most caudal point of the vocal processus of the left arytenoid	64	/
18	thyroid	semi	right apical ridge of the thyroid	1	19
19	thyroid	semi	right apical ridge of the thyroid	18	5
20	thyroid	semi	left apical ridge of the thyroid	1	21
21	thyroid	semi	left apical ridge of the thyroid	20	6
22	thyroid	semi	right lateral, connecting the upper and lower cornu	5	23
23	thyroid	semi	right lateral, connecting the upper and lower cornu	22	24
24	thyroid	semi	right lateral, connecting the upper and lower cornu	23	25
25	thyroid	semi	right lateral, connecting the upper and lower cornu	26	3
26	thyroid	semi	left lateral, connecting the upper and lower cornu	6	27
27	thyroid	semi	left lateral, connecting the upper and lower cornu	26	28
28	thyroid	semi	left lateral, connecting the upper and lower cornu	27	29
29	thyroid	semi	left lateral, connecting the upper and lower cornu	28	4
30	thyroid	semi	right lower ridge of the thyroid down to the lower right cornu	2	31
31	thyroid	semi	right lower ridge of the thyroid down to the lower right cornu	30	32
32	thyroid	semi	right lower ridge of the thyroid down to the lower right cornu	31	33
33	thyroid	semi	right lower ridge of the thyroid down to the lower right cornu	32	34
34	thyroid	semi	right lower ridge of the thyroid down to the lower right cornu	33	35
35	thyroid	semi	right lower ridge of the thyroid down to the lower right cornu	34	3
36	thyroid	semi	left lower ridge of the thyroid down to the lower left cornu	2	37
37	thyroid	semi	left lower ridge of the thyroid down to the lower left cornu	36	38
38	thyroid	semi	left lower ridge of the thyroid down to the lower left cornu	37	39
39	thyroid	semi	left lower ridge of the thyroid down to the lower left cornu	38	40
40	thyroid	semi	left lower ridge of the thyroid down to the lower left cornu	39	41
41	thyroid	semi	left lower ridge of the thyroid down to the lower left cornu	40	4

42	cricoid	semi	right upper ridge of the cricoid	8	43
43	cricoid	semi	right upper ridge of the cricoid	42	44
44	cricoid	semi	right upper ridge of the cricoid	43	10
45	cricoid	semi	left upper ridge of the cricoid	9	46
46	cricoid	semi	left upper ridge of the cricoid	47	49
47	cricoid	semi	left upper ridge of the cricoid	46	11
48	arytenoid	semi	lateral ridge of the right arytenoid	12	49
49	arytenoid	semi	lateral ridge of the right arytenoid	48	50
50	arytenoid	semi	lateral ridge of the right arytenoid	49	51
51	arytenoid	semi	lateral ridge of the right arytenoid	50	14
52	arytenoid	semi	lateral ridge of the right arytenoid	15	53
53	arytenoid	semi	lateral ridge of the right arytenoid	52	54
54	arytenoid	semi	lateral ridge of the right arytenoid	53	55
55	arytenoid	semi	lateral ridge of the right arytenoid	54	16
56	arytenoid	semi	lateral ridge of the left arytenoid	13	57
57	arytenoid	semi	lateral ridge of the left arytenoid	56	58
58	arytenoid	semi	lateral ridge of the left arytenoid	57	59
59	arytenoid	semi	lateral ridge of the left arytenoid	58	15
60	arytenoid	semi	lateral ridge of the left arytenoid	15	61
61	arytenoid	semi	lateral ridge of the left arytenoid	60	62
62	arytenoid	semi	lateral ridge of the left arytenoid	61	63
63	arytenoid	semi	lateral ridge of the left arytenoid	62	17
64	thyroid	semi	thyroid midline, which connects the two laminae	1	63
65	thyroid	semi	thyroid midline, which connects the two laminae	64	66
66	thyroid	semi	thyroid midline, which connects the two laminae	65	67
67	thyroid	semi	thyroid midline, which connects the two laminae	66	2

Symmetrization, Procrustes Analysis, and Principal Component Analysis:

After loading the landmark data into R and visually inspecting all extracted landmarks, the laryngeal landmark data was symmetrised. The larynx itself is a symmetrical organ in vivo, yet excised larynges can appear asymmetrical if excised and scanned ex vivo. I used the symmetrize() command from the Morpho package in R Studio for all landmarks (Version 1.4.1106; Schlager, Jefferis, Ian & Schlager, 2021). I used the function GPA from the Morpho package to run a general Procrustes analysis and scale, rotate, and orient all landmark sets, leaving pure shape information (Schlager, Jefferis, Ian & Schlager, 2021). Sliding (semi) landmarks were included with a step size of 0.1. This was a necessary choice to avoid unrealistic sliding due to immense shape differences. The adjusted data was then examined using through a principal component analysis (PCA), identifying four components capturing the main shape deformations across species. These PCA axes were then further used in identify the main allometric and phylogenetic relationships across morphological changes to the larynx.

Allometry:

To investigate the relationship between laryngeal centroid size and laryngeal shape I used a shape regression including the shape coordinates as a response variable and centroid size as a predictor. The laryngeal centroid size is a measure of overall size, which is obtained by calculating the square root of the sum of squared distances across all landmarks from their center of gravity (computed as the average landmark position across all landmarks) (Mitteroecker, 2020). I first ran this shape regression without taking phylogeny into account and then reran the analysis with the inclusion of phylogeny. I further tested for correlations between principal component scores 1 to 3 and centroid size.

Phylogenetic Analysis:

100 Phylogenetic trees with branch lengths scaled to time were downloaded for the species in our sample from VertLife.org (http://vertlife.org/phylosubsets). This block of trees is a taxonomic subset of an all-mammal supermatrix tree constructed based on 31 genes (27 nuclear and four mitochondrial) (Upham et al. 2019). From these 100 trees, which had identical topologies and differed only minimally in branch lengths, a consensus tree (fig. 1) was constructed using 'consensus.edges()' in the R package 'phytools' (Revell 2012). The topology and node ages of this consensus phylogeny for our thirteen species matches that from previously constructed phylogenetic relationships and divergence times (Agnarsson & May-Collado 2008; Derous et al. 2021; O'Leary & Gatesy 2008; Price et al. 2005)

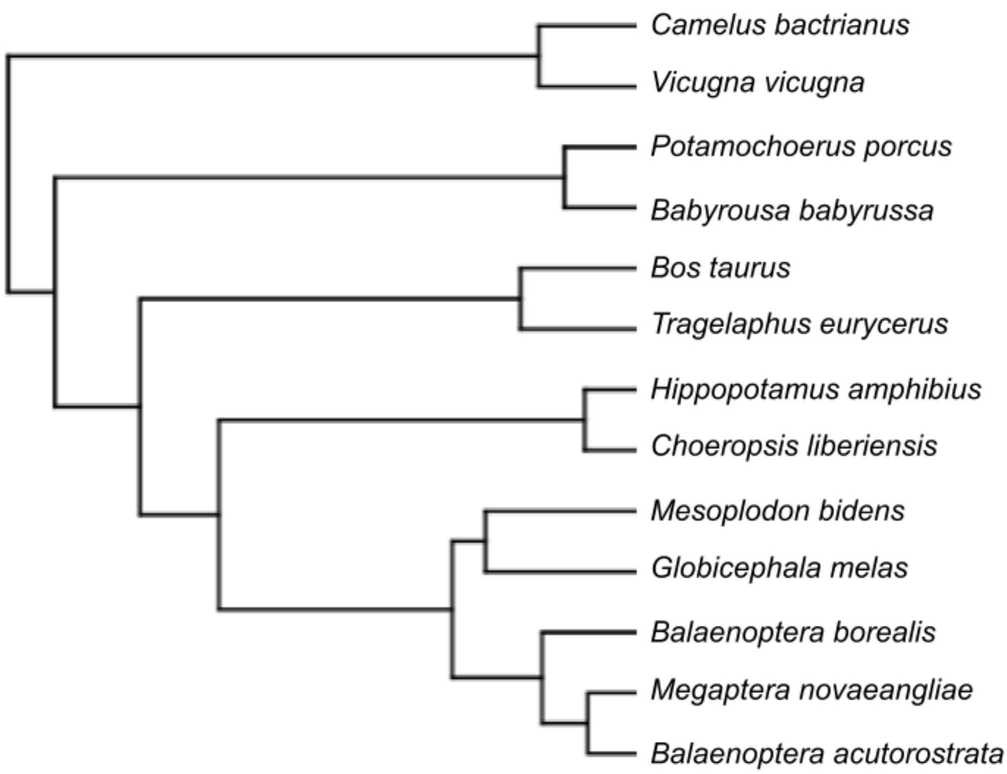

Figure 4: Consensus tree with branch lengths scaled to time for the 13 cetartiodactylan species used in this study. Based on 100 RAxML trees downloaded from VertLife.org (Upham et al. 2019).

Phylogenetic signal measures the statistical dependency of certain trait values in different species due to how they are phylogenetically related to one another (Blomberg, Garland & Ives 2003; Pagel 1997; 1999). The most common forms are either Blomberg's K or Pagel's lambda, with Blomberg's K focusing on the variances among the species over the variances of contrasts. It is a scaled ratio, while Pagel's lambda is a scaling factor, that shows the correlations between the species in relation to the correlation that would be expected under Brownian evolution. In the case of Pagel's lambda, when the value is approaching 1 this would mean a consistency with Brownian evolution, whereas if the value is closer to 0, independent trait evolution can be expected, i.e., the trait cannot be explained by phylogeny, but underlies other factors. For Blomberg's K, one can interpret a value bigger than one as having found a stronger phylogenetic signal than expected under Brownian Motion, while a value smaller than 1 suggests that the traits one is looking at vary along the phylogeny in a random manner. In the case of this study, it was decided to include both options, leaving more room for interpretation and comparison later on.

Results:

Principal Component Analysis:

In the Principal Component Analysis, the first four components accounted for 84.6% of the total variation. PC1, capturing the shape of the thyroid shield, as well as the opening/closing of the cricoid ring, accounted for 40.3% of variance (fig. 2). The second component explained 22.3% of the total variation, likely capturing the shape and length of the upper and lower arytenoid processes as well as the upper thyroid ridge (fig. 2). The third and fourth component are associated with subtler morphological features. PC3 explains 16.8% and captures the angle of the upper cricoid ridge, as well as thyroid shape (bulbous vs elongated; fig. 3). PC4 captures 5.2% of variance and is associates with the thickness of the lower thyroid processes (fig. 3). Component 1 and 3 plotted against one another (fig. 4), show the strongest differences between aquatic and terrestrial artiodactyls, with the whales plotting in the lower right quadrant of the coordinate system. This underlines the similarities between cetacean larynges, compared to their terrestrial relatives, which show a greater variation across component 1 and 3. These clusters across components further support the idea that laryngeal shape is strongly correlated with adaptations to a fully aquatic life. The semi aquatic hippo and pygmy hippo showed obvious similarities with the cetaceans in component 3, but other than that clustered close to the terrestrials.

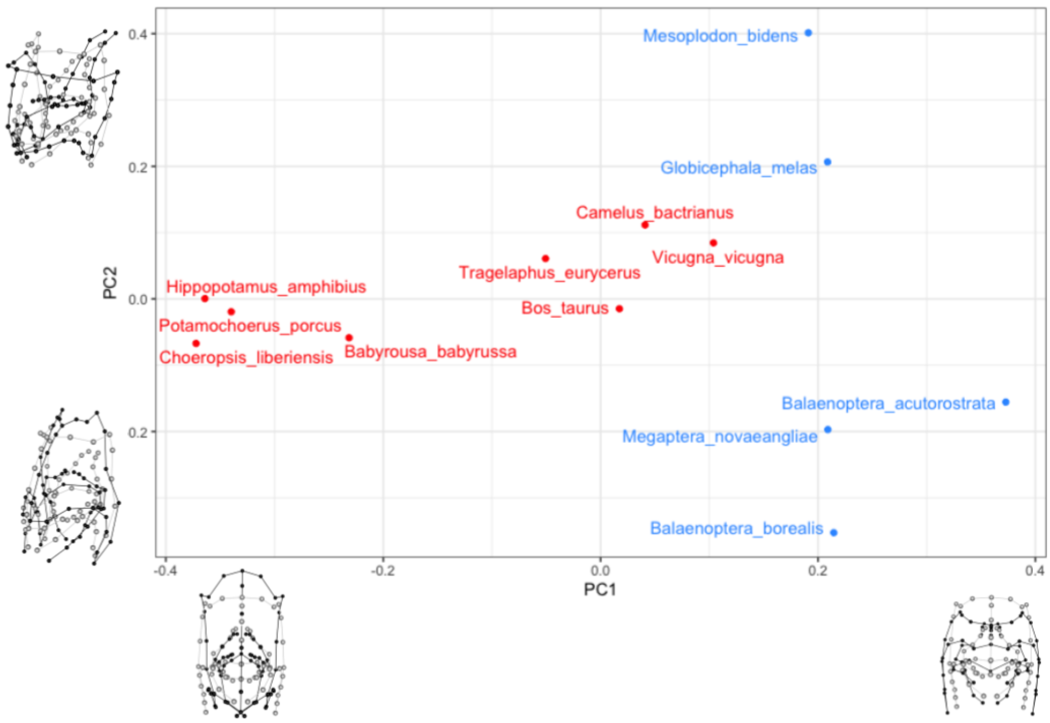

Figure 5: The Principal Component analysis plot of PC1 against PC2 for all specimens. PC1 is associated with the thyroid shape, as well as the cricoid being open ventrally or closed and accounts for 40.3% of the total variation. PC2 explains 22.3% and associates with the different processes of the arytenoids. Terrestrial and semi-aquatic species are shown in red, cetaceans in blue.

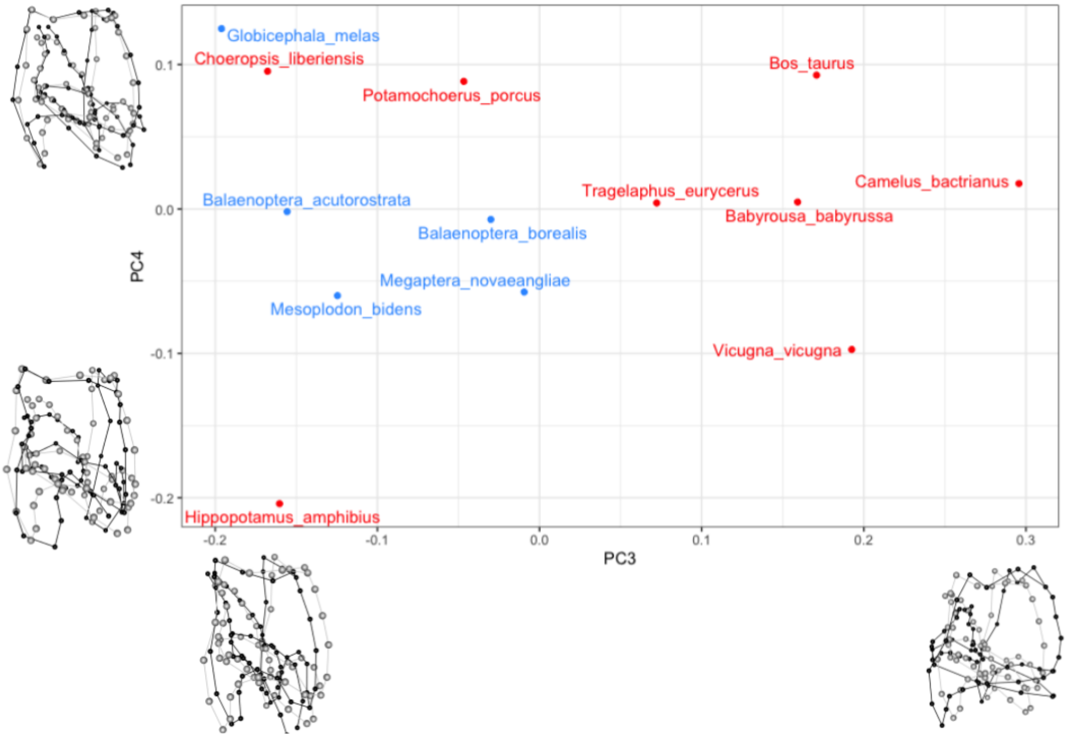

Figure 6: The Principal Component analysis plot of PC3 against PC4 for all specimens. PC3 is associated with the angle of the upper cricoid ridge, it accounts for 16.8% of the total variation. PC4 explains 5.2% and associates with the wideness of the lower thyroid processes. Terrestrial and semi-aquatic species are shown in red, cetaceans in blue.

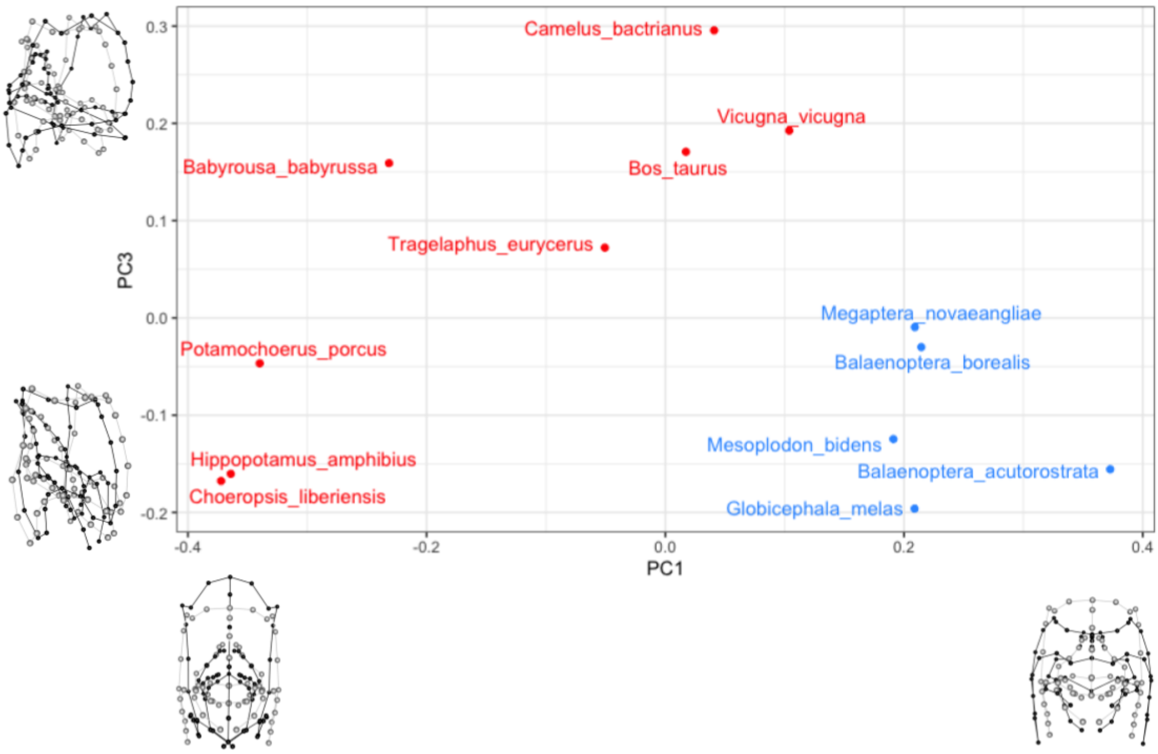

Figure 7: The Principal Component analysis plot of PC1 against PC3 for all specimens. PC1 is associated the thyroid shape, as well as the cricoid being open ventrally or closed and accounts for 40.3% of the total variation. Terrestrial and semi-aquatic species are shown in red, cetaceans in blue. PC3 explains the angle of the upper cricoid ridge, it accounts for 16.8%.

Allometry:

I found a possible positive correlation between PC 1 and the laryngeal centroid size CS (cor = 0.5317; p-value = 0.0614), which potentially is connected to the fact that general shape traits captured in component 1 most strongly capture cetacean adaptations (e.g. open cricoid; fig. 5). These traits also happen to coincide with cetaceans being on average much larger than typical terrestrial artiodactyls. Figure 5 illustrates the hippo as an outlier compared to terrestrial artiodactyls. It is more similar to cetaceans in regard to centroid size yet clusters lower on component 1.

I did not find a strong relationship between component 2 and centroid size (cor = -0.3250; p-value = 0.2785; fig. 6), but component 3 and centroid size are correlated negatively (cor = -0.5602; p-value = 0.04645; fig. 7).

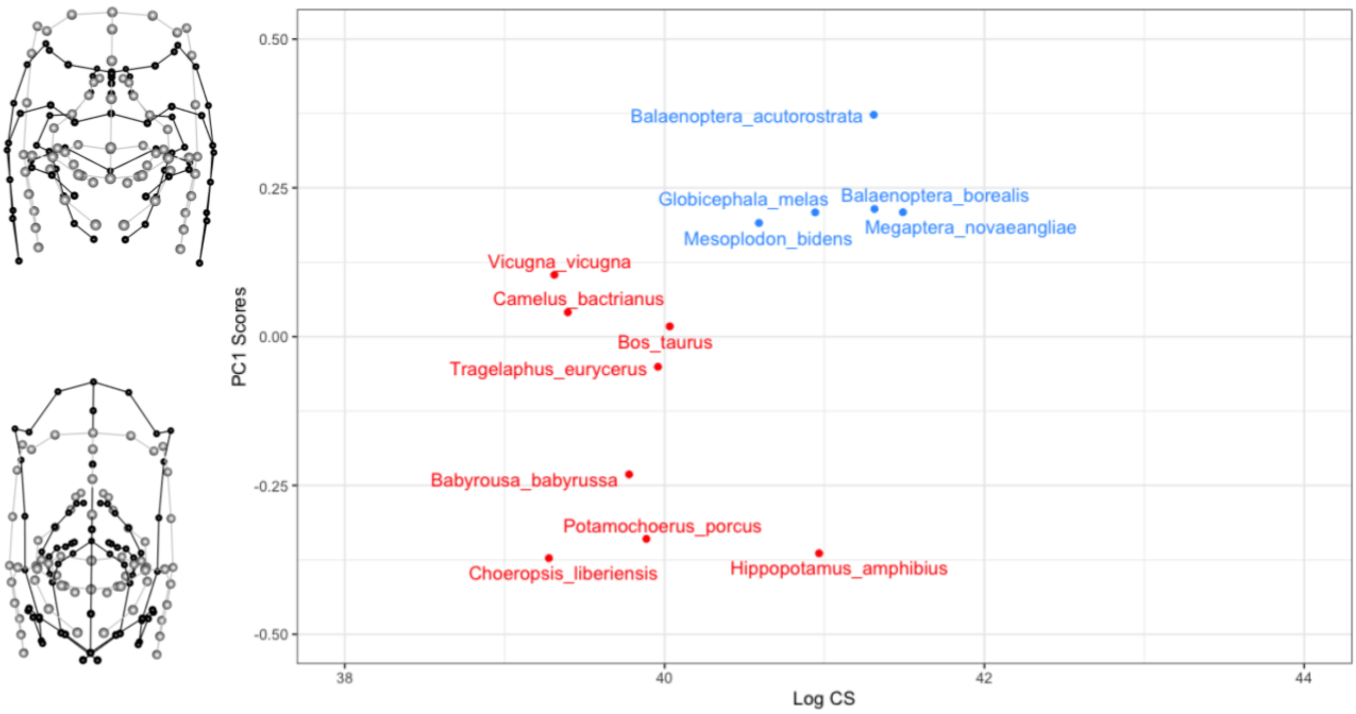

Figure 8: The relationship between the PC1 scores and the centroid size is depicted. Cetaceans are displayed in blue, quadrupeds in red. The X-axis displays the log centroid size (CS), on the Y-axis are the PC1 Scores from the principal component analysis.

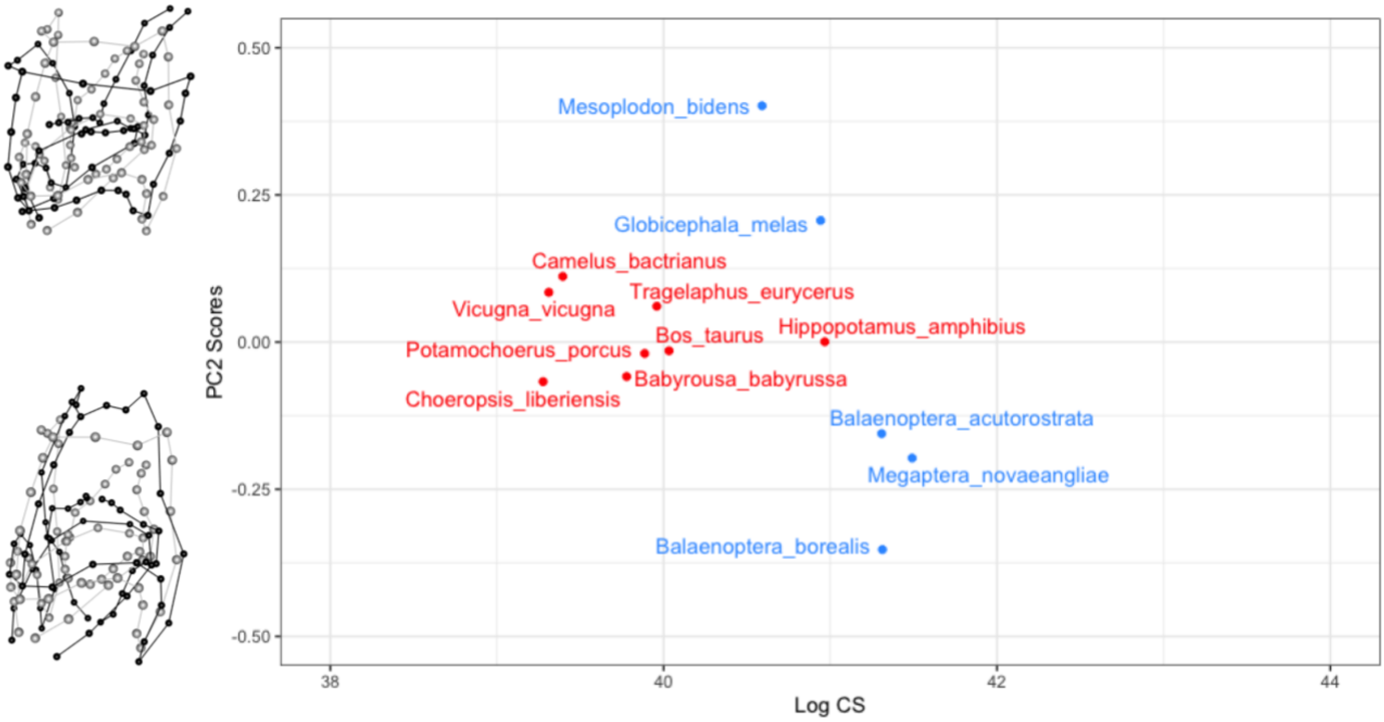

Figure 9: The relationship between the PC2 scores and the centroid size is depicted. Cetaceans are displayed in blue, quadrupeds in red. The X-axis displays the log centroid size (CS), on the Y-axis are the PC2 Scores from the principal component analysis.

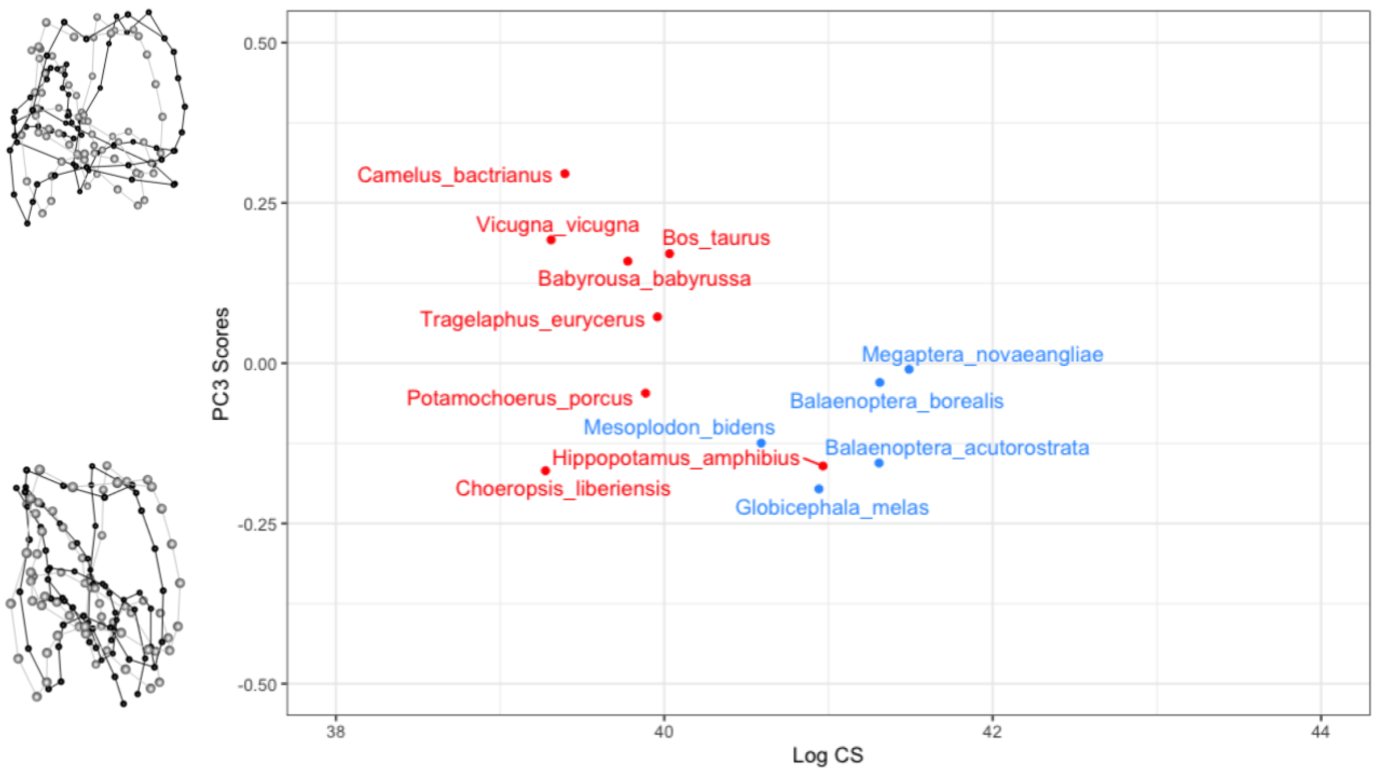

Figure 10: The relationship between the PC3 scores and the centroid size is depicted. Cetaceans are displayed in blue, quadrupeds in red. The X-axis displays the log centroid size (CS), on the Y-axis are the PC3 Scores from the principal component analysis.

Phylogenetic signal in the Principal Components:

Blomberg's K and Pagel's lambda were both were used to assess the influence of phylogeny on shape. The two measures of phylogenetic signal indicated the following results across PC scores: The highest concentration of laryngeal shape data was found to be concentrated in components 1 to 3. More specifically a Pagel score of 0.9999 with a p-value < 0.001, therefore highly significant, suggests a very strong connection of the traits captured in component 1 to be of phylogenetic (evolutionary) origin. A Blomberg's K score of 1.501 (p-value = 0.001), further is in line with the Brownian motion and supports the notion of these morphological changes being of evolutionary origin. Another significant relation was found for PC3 in both Pagel's lambda (lambda = 0.8160, p-value = 0.015) and Blomberg's K (0.8605, p-value = 0.007). The angle of the superior cricoid ridge, as well as the elongatedness of a cetartiodactylan larynx is highly dependable on phylogeny.

Table 3: Displayed are the results of testing for Blomberg's K.

	Blomberg's K	p-value
PC1	1.501	0.001
PC2	0.5011	0.069
PC3	0.8605	0.007
PC4	0.1825	0.921

Table 4: Displayed are the results of testing for Pagel's lambda.

	Pagel's lambda	p-value
PC1	0.9999339	0.00041478
PC2	0.0000661	1
PC3	0.8160534	0.015441
PC4	0.0000661	1

Phylogenetic signal in allometric testing:

Adding to the allometric tests from before, I further investigated the allometric relationship between centroid size (CS) and the Procrustes shape coordinates, i.e. laryngeal shape, using shape regression (both including and excluding phylogeny). The shape regression excluding phylogeny explained a variation of 19% (Rsq = 0.1966, p = 0.025). This would indicate centroid size to be a significant predictor of shape. After rerunning this shape regression with phylogeny considered, I found variance explained by centroid size to drop to 11.2% of the total variation in laryngeal shape (Rsq = 0.11212, p = 0.166).

Discussion:

The evolutionary adaptation made by cetaceans from life on land to a fully aquatic life comes with drastic changes in all morphological aspects. Limbs turn to fins, tails evolve flukes, and even structurally conservative organs like the larynx evolve to best fulfil its functions in a completely different environment. The aim of this study was to quantify changes to laryngeal morphology while taking phylogeny into account. I provide a first overview of how different environments (aquatic, semi aquatic, and terrestrial) affect the dimension and shape of laryngeal morphology. One core aspect of this study is the finding that shape adaption to an aquatic life is captured first and foremost by an opening of the cricoid cartilage and of the thyroid cartilage; both changes are captured in component 1 of my component analysis and explain 40.3% of shape variation, heavily associated with phylogeny.

Laryngeal shape variation across cetartiodactyls is quite impressive, especially when comparing whales and terrestrial artiodactyls. Whales and terrestrial artiodactyls differ most in the shape of the thyroid shield, as well as whether the cricoid is ring-shaped or ventrally open (PC1). The cetacean thyroid shield covers only the caudal part of the larynx in cetaceans, leaving the open cricoid exposed on the rostral side. This, in mysticetes at least, is thought to be due to the air sacs taking up this space when inflated but would not be an explanation in odontocetes, since their air sacs are not positioned near the ventral thyroid (Reidenberg & Laitman 2008). However, in odontocetes the thyroid sits much closer to the cricoid than in mysticetes, where the space between the cartilages is much more prominent (Hosokawa, 1950; Reidenberg & Laitman, 1987, 2007). For previous research it would be interesting to have a toothed whale with a ring-shaped cricoid (e.g. sperm whale) as part of the sample for a similar study, or even focus solely on the matter of cricoid shape variation in toothed whales. An open cricoid potentially allows for more flexibility of the organ, which could more easily accommodate in “deflating” or “folding” of the organ under extreme water pressure while diving.

Cetaceans further have longer arytenoids in comparison to the arytenoids of the terrestrial artiodactyls, which tend to be more compact in size. I found here that in odontocetes the upper part of the arytenoid cartilages showed elongation, while in mysticetes it was the lower part (PC2). This may be connected to the different strategies in vocal fold (U-fold in mysticetes) angle the two sister groups developed. As it was discussed in the introduction of this paper, the mysticete U-fold and the odontocete vocal folds are situated parallel to the flow of air, but the groups differ in the direction the ventral attachment of the thyroid rotated towards, with in mysticetes displaying a rotation 90° downwards, and 90° upwards in odontocetes. This is especially interesting since it has been found that in certain pinnipeds, which are also secondarily aquatic, the vocal fold angle rotated as well towards a parallel position regarding the flow of air (Schneider 1964). In the case of the Californian Sea Lion (*Zalophus californianus*) and the grey seal (*Halichoerus grypus*), to name just two examples, the vocal folds display a similar pattern as can be found in the odontocetes due to an elongation of the arytenoid cartilages. On the other hand, in other pinnipeds, like the harbour seal (*Phoca vitulina*), the vocal folds sit perpendicular to the tracheal airflow, as can be found in terrestrial Artiodactyls. Research investigating the reason behind such a variety in vocal fold angle across one taxon might give a better understanding also about how this feature developed in cetaceans (Reidenberg, 2017; Schneider, 1963).

Previous research has described the semi-aquatic Hippopotamidae as a connecting link between the cetaceans and terrestrial Artiodacytla (Reidenberg, 2017). Not only are Hippopotamidae semi-aquatic but they also vocalize under water (Barklow, 2004) as do whales. It therefore seems plausible the hippopotamus and the pygmy hippopotamus laryngeal morphology should be situated between terrestrial artiodactyls and cetaceans. When analyzing certain functions that the larynx fulfills in the hippopotami as well as the cetaceans, we find many more similarities than just the fact that both vocalize underwater. The biggest similarity in the whippomorphs, the clade including whales and hippopotami, is the feature of having the epiglottis overlap with the soft palate. In both cases this serves to keep water from entering the air-passage-ways, a crucial adaptation to life in water. This feature is made even more efficient by the fact that the larynx is found to be reaching up into the naso-pharyngeal cavity and in the case of hippopotami and toothed whales being tightly interlocked in that position (Reidenberg 2017). Furthermore, the angle of the vocal folds in hippopotami approaches a position parallel to the airflow, a similar position to the situation found in mysticetes. Nonetheless, while functionality-wise the whippomorphs show many functional similarities, their laryngeal shape differs greatly along most of the principal component axes and shows no significant relation. In the case of the pygmy hippopotamus the difference is even greater than in the hippopotamus. These findings indicate that the hippopotamus larynx retained the traditional shape of the artiodactyls, despite regularly vocalizing under water. This underlines the unique route the Cetacea took in larynx adaptations.

Testing for a correlation between the centroid size (CS), a proxy for larynx size, and laryngeal shape in the form of the first principal components of the PCA, showed that the shape of the thyroid and the cricoid cartilage (PC1) is clearly positively correlated to the laryngeal centroid size. Other principal components showed no correlation with the larynx size in either direction. When taking phylogeny into consideration and again comparing CS and principal component 1, the correlation drops from 19,66% to 11.2% and loses significance. This indicates how important it is crucial to take phylogeny into account; Cetaceans, in addition to having adapted their larynx to an aquatic life, also happen to be some of the largest species of mammals, potentially distorting results ignoring phylogeny.

This can also be read from the results of Pagel's lambda and Blomberg's K. The thyroid- and cricoid shape of the PC1 axes in both tests underlies significantly the phylogenetic signal, as well does the angle of the upper cricoid ridge associated with PC3. There was no such clear signal in features like the length of the arytenoids/ arytenoid-corniculate-complex (PC2) or the shape and thickness of the lower thyroid processes. Those components show very little to no consistency with the Brownian motion model, therefore cannot be explained by phylogeny and would be subject to other shape determining pressures, like adaptations to environmental conditions.

Some ambiguity in the results of this study, in the form of certain outliers, could have several explanations, the age of certain specimen being the most relevant. The older a specimen, the more calcified its larynx, making the organ more rigid and preventing it from crushing beneath its own weight, which influences CT-scanning along with the making of the models in Amira and therefore the positions of the landmarks. Some of the specimen in this sample, terrestrials as well as whales were young, resulting in a less mineralized (and smaller, potentially not fully developed) larynx. In the case of the pygmy hippopotamus (*Choeropsis liberiensis*) and the Bactrian camel (*Camelus bactrianus*) even two neonates were included. The pygmy hippopotamus is especially interesting therefore, since it was found to be unexpectedly far from its closest relative, the hippopotamus (*Hippopotamus amphibius*), which positioned itself closer to the whales (fig. 5-7). To a certain degree this is not relevant for this study, since most of the laryngeal variation is to be found between terrestrial and aquatic cetartiodactyls. In future research, it would be interesting to further explore the morphological differences between the hippopotamus and the pygmy hippopotamus and whether the corresponding results of this study are mainly based in the underdeveloped state of our pygmy hippopotamus' specimen, or represent real biological differences.

Another point worth discussing is the scanning process and how it affected the shape of the larynx reconstructions. Whale larynges tended to be less rigid and/or mineralized than the other specimen. This may be simply due to the age of the animals or may reflect greater flexibility for coping with pressure increases during deeper dives. So, when laid atop the scanning surface of the CT-scanner, the cetacean larynx deformed more strongly under its own weight. I suspect that this affects the analysis minimally, especially since the extra step of landmark-symmetrization was undertaken to counter these distortions.
Much of the previous research has focused on the laryngeal changes in whales through simple dissections. But using the method of geometric morphometrics especially, provides an interesting opportunity to identify precisely and quantitatively which cartilages and which of their characteristics have been impacted the most by an aquatic or semi aquatic lifestyle

References:

Adams, D. C., & Otárola-Castillo, E. (2013). Geomorph: An r package for the collection and analysis of geometric morphometric shape data. *Methods in Ecology and Evolution*, *4*(4), 393–399. https://doi.org/10.1111/2041-210X.12035

Agnarsson I, May-Collado LJM (2008). The phylogeny of Cetartiodactyla: The importance of dense taxon sampling, missing data, and the remarkable promise of cytochrome b to provide reliable species-level phylogenies. *Molecular Phylogenetics and Evolution* 48(3), 964-985.

Barklow, W. E. (2004). Amphibious communication with sound in hippos, Hippopotamus amphibius. *Animal behaviour*, *68*(5), 1125-1132.

Benham, W. B. (1901). On the larynx of certain whales (Kogia, Balaenoptera and Ziphius). *Proceedings of the Zoological Society (London), 1*, 286-300.

Blomberg, S. P., Garland Jr, T., & Ives, A. R. (2003). Testing for phylogenetic signal in comparative data: behavioral traits are more labile. *Evolution*, *57*(4), 717-745.

Derous D, Sahu J, Douglas A, Lusseau D, Wenzel M (2021). Comparative genomics of cetartiodactyla: energy metabolism underpins the transition to an aquatic lifestyle. *Conservation Physiology* 9(1), coaa136.

Fitch, W.T. (2016). Vertebrate bioacoustics: Prospects and open problems. In Suthers, R.A. (Ed.) *Vertebrate Sound Production and Acoustic Communication*. New York: Springer, pp. 297-328.

Gunz, P., & Mitteroecker, P. (2013). Semilandmarks: A method for quantifying curves and surfaces. *Hystrix*, *24*(1), 103–109. https://doi.org/10.4404/hystrix-24.1-6292

Hosokawa, H. (1950). On the cetacean larynx, with special remarks on the laryngeal sack of the sei whale and the aryteno-epiglottideal tube of the sperm whale. *Scientific Reports of the Whales Research Institute*, *3*(8), 23–62.

Loth, A., Corny, J., Santini, L., Dahan, L., Dessi, P., Adalian, P., & Fakhry, N. (2015). Analysis of hyoid–larynx complex using 3D geometric morphometrics. *Dysphagia*, *30*(3), 357-364.

Mitteroecker, P. (2020). Morphometrics in Evolutionary Developmental Biology. *Evolutionary Developmental Biology*, 1–11. https://doi.org/10.1007/978-3-319-33038-9_119-1

Molina-Venegas, R., & Rodríguez, M. Á. (2017). Revisiting phylogenetic signal; strong or negligible impacts of polytomies and branch length information?. *BMC evolutionary biology*, *17*(1), 1-10.

O'Leary MA, Gatesy J (2008). Impact of increased character sampling on the phylogeny of Cetartiodactyla (Mammalia): combined analysis including fossils. *Cladistics* 24(4), 397-442.

Pagel, M. (1997). Inferring evolutionary processes from phylogenies. *Zoologica Scripta*, *26*(4), 331-348.

Pagel, M. (1999). Inferring the historical patterns of biological evolution. *Nature*, *401*(6756), 877-884.

Price SA, Bininda-Emonds ORP, Gittleman JL (2005). A complete phylogeny of the whales, dolphins and even-toed hoofed mammals (Cetartiodactyla). *Biological Reviews* 80, 445-473.

Reidenberg, J. S. (2017). Terrestrial, semiaquatic, and fully aquatic mammal sound production mechanisms. *Acoutics Today*, *13*(2), 35–43.

Reidenberg, J. S., & Laitman, J. T. (1987). Position of the larynx in odontoceti (toothed whales). *The Anatomical Record*, *218*(1), 98–106. https://doi.org/10.1002/ar.1092180115

Reidenberg, J. S., & Laitman, J. T. (1988). Existence of vocal folds in the larynx of odontoceti (toothed whales). *The Anatomical Record*, *221*(4), 884–891. https://doi.org/10.1002/ar.1092210413

Reidenberg, J. S., & Laitman, J. T. (2007). Discovery of a low frequency sound source in Mysticeti (baleen whales): Anatomical establishment of a vocal fold homolog. *The Anatomical Record*, *209*(6), 745–759.

Reidenberg, J. S., & Laitman, J. T. (2008). Sisters of the sinuses: cetacean air sacs. *The Anatomical Record: Advances in Integrative Anatomy and Evolutionary Biology: Advances in Integrative Anatomy and Evolutionary Biology*, *291*(11), 1389-1396.

Revell LJ (2012). phytools: An R package for phylogenetic comparative biology (and other things). Methods in Ecology & Evolution 3, 217-223.

Richtsmeier, J. T., Burke Deleon, V., & Lele, S. R. (2002). The promise of geometric morphometrics. *American Journal of Physical Anthropology: The Official Publication of the American Association of Physical Anthropologists*, *119*(S35), 63-91.

Schlager, S., Jefferis, G., Ian, D., & Schlager, M. S. (2019). Package 'Morpho'.

Schneider, R. (1963). *Morphologische Anpassungserscheinungen am Kehlkopf einiger aquatiler Säugetiere*.

Schneider, R., & Kükenthal, W. G. (1964). *Der larynx der säugetiere*. de Gruyter.

Schoenfuss, H. L., Bragulla, H. H., Schumacher, J., Henk, W. G., Craig George, J., & Hillmann, D. J. (2014). The anatomy of the larynx of the bowhead whale, Balaena mysticetus, and its sound-producing functions. *Anatomical Record*, *297*(7), 1316–1330. https://doi.org/10.1002/ar.22907

Titze, I.R. (1994). *Principles of Voice Production*. Prentice Hall.

Upham NS, Esselstyn JA, Jetz W (2019). Inferring the mammal tree: Species-level sets of phylogenies for questions in ecology, evolution, and conservation. *PLoS Biology* 17(12), e3000494.